

## *International Journal of Scientific Research and Reviews*

### **Influence of Precursor Concentration on CBD grown ZnO Thin Films**

**Vipul Shukla\*and Amit Patel**

\*Gujarat Technological University, Chandkheda, Ahmedabad –382 424 Gujarat,India

Government Engineering college, Godhra –389 001 Gujarat,India

\*Email: [vipuljshukla317@gmail.com](mailto:vipuljshukla317@gmail.com)

#### **ABSTRACT**

ZnO thin films are deposited on glass substrate from aqueous solution of  $ZnCl_2$  and  $NH_3$  by chemical bath deposition. The films of various thicknesses, particle size and other useful analysis have been obtained by varying the concentration of  $ZnCl_2$  from 0.1M, 0.2M, 0.3M, 0.4M and 0.5M. Optical properties of grown films and influence of precursor concentration on them are analyzed by the transmittance recorded in the range 200-1200 nm. Deposited films are also characterized by X-ray diffraction and SEM to understand the influence of variation in precursor concentration on structural and morphological properties of grown films. XRD patterns confirmed the hexagonal wurtzite structure of the deposited ZnO films.

**KEYWORDS:** ZnO, Chemical bath deposition, XRD, UV-Vis-NIR, SEM.

**\*Corresponding author**

**Vipul Shukla**

Gujarat Technological University, Chandkheda, Ahmedabad –382 424 Gujarat,India

Government Engineering college, Godhra –389 001 Gujarat,India

Email: [vipuljshukla317@gmail.com](mailto:vipuljshukla317@gmail.com)

## INTRODUCTION

Increasingly, zinc oxide is attracting researchers due to its unique properties and the possibility of its application as base material in a variety micro-, optical- and acoustic-electronic devices. This material has high transparency in the visible spectrum, low toxicity, chemical and thermal stability, and good biocompatibility<sup>[1]</sup>. Moreover, due to its high exciton-binding energy (60 meV), effective laser generation is expected at room temperature<sup>[2]</sup>. Also, ZnO has a large band gap ( $E_g = 3.37$  eV); consequently, it effectively absorbs ultraviolet radiation and so can be used as a sensor of UV radiation<sup>[3]</sup>. Furthermore, ZnO films are widely used as conductive- and window-layers of large-area solar cells<sup>[4]</sup>. Numerous growth techniques have been used to produce ZnO thin films including molecular-beam epitaxy<sup>[5]</sup>, vapor deposition<sup>[6]</sup>, magnetron sputtering<sup>[7]</sup>, spray pyrolysis<sup>[8]</sup>, and the sol-gel method<sup>[9]</sup>. Most of these processes are characterized by high complexity, and they necessitate use of high vacuum, energy or temperature during synthesis. Nowadays, chemical bath deposition (CBD)<sup>[10]</sup> is one of the most promising methods for obtaining ZnO films. It is widely used for deposition of various metal chalcogenide thin films. It produces good deposits on suitable substrates by the controlled precipitation of compounds from the solution. The method offers many advantages over other well-known vapor phase synthesis routes. It may allow us to easily control the growth factors such as film thickness, deposition rate and quality of crystallites by varying the solution pH, temperature and bath concentration<sup>[11]</sup>. It does not require high voltage/vacuumequipment, works at room temperature, and hence it is inexpensive. The only requirement for this deposition route is an aqueous solution consisting of a few common chemicals and a substrate for the film to be deposited. Its main advantages are simplicity and efficiency, requiring only relatively low temperature during synthesis, and, also affording the possibility of obtaining of large-areal layers on substrates of different shapes. It often suffers from a lack of reproducibility in comparison with other chemical processes; however, by the proper and careful optimization of the growth parameters, one can achieve reasonable reproducibility. In the present work, we report properties of ZnO thin films deposited by bath consisted of equal volumes of zinc chloride( $ZnCl_2$ ) solutions having concentrations varying from 0.1 M to 0.5 M.

## EXPERIMENTAL PROCEDURE

### *Synthesis of ZnO*

ZnO thin films are synthesized by CBD method from aqueous solution of  $ZnCl_2$  anhydrous as precursor. Commercial quality microscope glass slides of dimension 25 mm x 75 mm x 1 mm are used as substrate. Prior to deposition, substrates were soaked in a concentrated HCl for 24 hours. After that they were washed thoroughly in cold detergent solution, rinsed in distilled water,

ultrasonicated in methanol for 15 minutes and dried at 50 °C in oven, to affirm proper degreased and clean substrate surface.

Reagents used in this experiment are zinc chloride anhydrous and aqueous ammonia. 0.1 M, 80 ml aqueous solution of zinc chloride was prepared. In this solution aqueous ammonia was added drop wise; while stirring the solution continuously to make the pH of solution to 9.6. After that, solution was transferred to a 100 ml beaker and kept in a constant temperature water bath with the substrate immersed vertically in the solution. Temperature of the bath was maintained at 80 °C. Slowly the clear solution starts turning in to turbid one which confirms the starting of thin film deposition. Substrate was kept in the bath for 120 minutes, after which it was removed from the bath, rinsed with distilled water, and dried at 50 °C in oven. Thin films obtained after drying were annealed at 500 °C for 2 hours to affirm their conversion in to ZnO.

Using same experimental method ZnO thin films were prepared for various concentrations 0.2M, 0.3M, 0.4M and 0.5M respectively.

### ***Measuring Instruments***

Thin films were characterized for structure, morphology and optical properties. Structural parameters of thin films are analyzed using powder XRD by patterns recorded with D<sub>2</sub>phaserBruker advanced X-ray diffractometer using a Cu - K $\alpha$  radiation source ( $\lambda = 1.547 \text{ \AA}$ ). Diffraction peaks were compared with those of the standard compounds reported in the JCPDS files. Surface morphologies of thin films were studied by scanning electron microscope (SEM) JSM-6010LA. UV-Vis-NIR absorption spectra of thin films were recorded in the wave length range of 200-1200 nm using a Shimadzu UV-3600 UV-Vis-NIR spectrometer.

## **RESULTS AND DISCUSSION**

### ***X-ray diffraction analysis***

X-ray diffraction (XRD) patterns of ZnO thin films deposited on glass substrate for different solution concentrations from 0.1 M to 0.5 M are shown in Fig.1. A matching of observed and standard 'd' values of ZnO using JCPDS card No. 36-1451 confirms the deposited films fit well with hexagonal wurtzite structure. XRD patterns exhibit strong peaks (100), (002), (101), (102), (110), (103) and (200) planes assigned to hexagonal wurtzite structure.

.

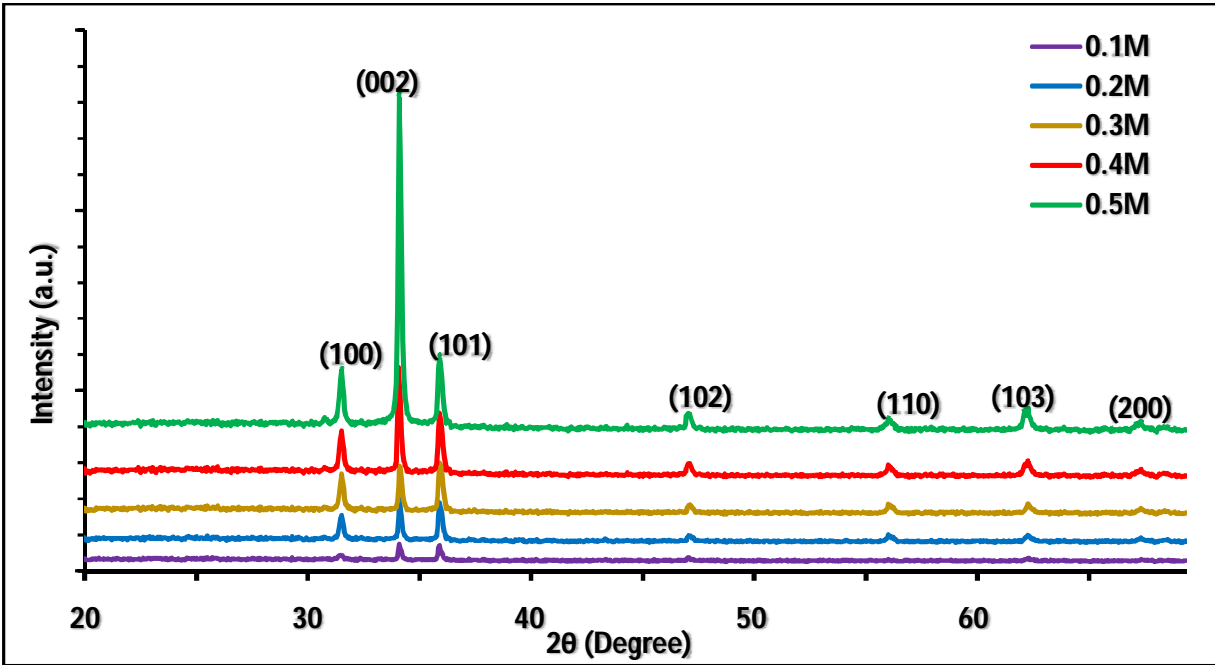


Figure 1. Powder XRD patterns for variation in precursor concentration ZnO thin films.

It can be seen from the XRD data that all samples are of single phase ZnO wurtzite structure (JCPDS, 36-1451), and the crystallinity of the films becomes better with increasing concentration. Diffraction peaks corresponding to the impurity were not found in the XRD patterns, confirming the high purity of the synthesized products.

The crystallite size of the ZnO nanoparticles was calculated by the X-ray line broadening method using the Scherrer's equation<sup>[12]</sup>:

$$D = \frac{K\lambda}{\beta \cos \theta} \quad (1)$$

Where D is the crystallite size,  $\lambda$  is the Cu-K $\alpha$  radiation of wavelength (1.547Å), K the shape factor 0.94,  $\beta_{hkl}$  is the full width at half maximum (FWHM) in radian and  $\theta$  is the scattering angle.

The dislocation density ( $\delta$ ), defined as the length of dislocation lines per unit volume. The dislocation density was calculated by the relation<sup>[13]</sup>:

$$\delta = \frac{1}{D^2} \quad (2)$$

Where D is the grain size.

The micro strain of the thin films is estimated using the equation<sup>[14]</sup>:

$$\varepsilon = \frac{\beta \cos \theta}{4} \quad (3)$$

Where, A is absorbance and t is the thickness. Shakti (2010) notes that the absorption coefficient  $\alpha$  and the extinction coefficient k are related by the formula (Shaaban E.R., 2006)<sup>[15]</sup>

$$K = \frac{\alpha\lambda}{4\pi} \quad (4)$$

The average value of grain size, refractive indices, extinction coefficient, the dislocation density ( $\delta$ ) and the micro strain ( $\epsilon$ ) are presented in table 1.

### ***Morphological analysis***

The morphologies of the deposited materials were examined using scanning electron microscopy. The films deposited under the optimized conditions were smooth and uniformly covered the substrate with good adherence. The following fig. show the surface morphology of the ZnO nanostructures grown with different concentrations i.e. 0.1mol/L, 0.2mol/L, 0.3mol/L, 0.4mol/L and 0.5mol/L. The preparation of ZnO nanorods was the pure hexagonal wurtzite structure(fig.2c). It exhibits well defined grain edges, and the inset shows a magnified view of individual grains. The overall surface structure is seen to have grains of hexagonal shape, uniformly covering the substrate, without any cracks or pores.

It can be seen from the above figure the concentration had a great influence on the morphology of the ZnO thin films. The length of the ZnO crystals is 2.7  $\mu\text{m}$  and the average diameter is 180 nm, when the reactant concentration is 0.1mol/L. For 0.4mol/L, the thickness of the film is 3.39  $\mu\text{m}$ . With the increasing concentration of  $\text{ZnCl}_2$  up to 0.5mol/L, the length of ZnO nanorods increases up to 1177 nm(fig.2d) and the diameter is also increased gradually up to 850 nm. From the figure, it can be seen that the specific surface area was gradually increased with the increasing of the concentration of reactants. Therefore, it can be concluded that the sizes of ZnO hexagonal wurtzite structure depend on the concentration of reactants, which can lead to the products with different length and diameters.

Table 1 indicates the thickness of the film, as the concentration of the precursor increases thickness of the film is also increases from 1.14  $\mu\text{m}$  to 10.20  $\mu\text{m}$ (Table 1).Fig.2 (e) shows complete growth mechanism of ZnO hexagonal wurtzite structure from stage 1 to stage 6, means from initial to final stage.

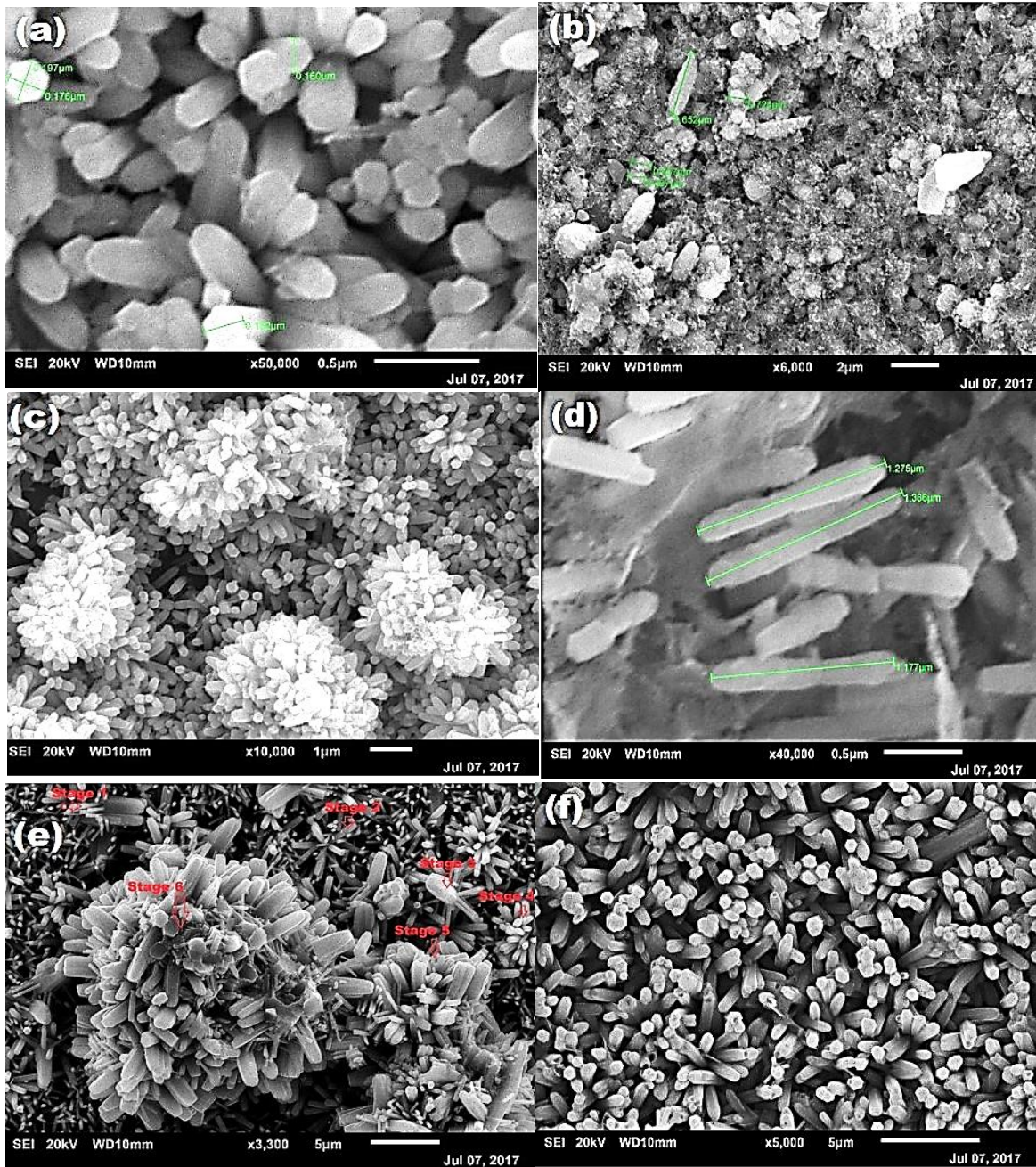


Fig.2a to 2f SEM images of the ZnO hexagonal wurtzite structure film

Cross-sectional SEM micrographs shown in figure 3 indicate the increase in thickness of ZnO thin film with variation in precursor concentration.

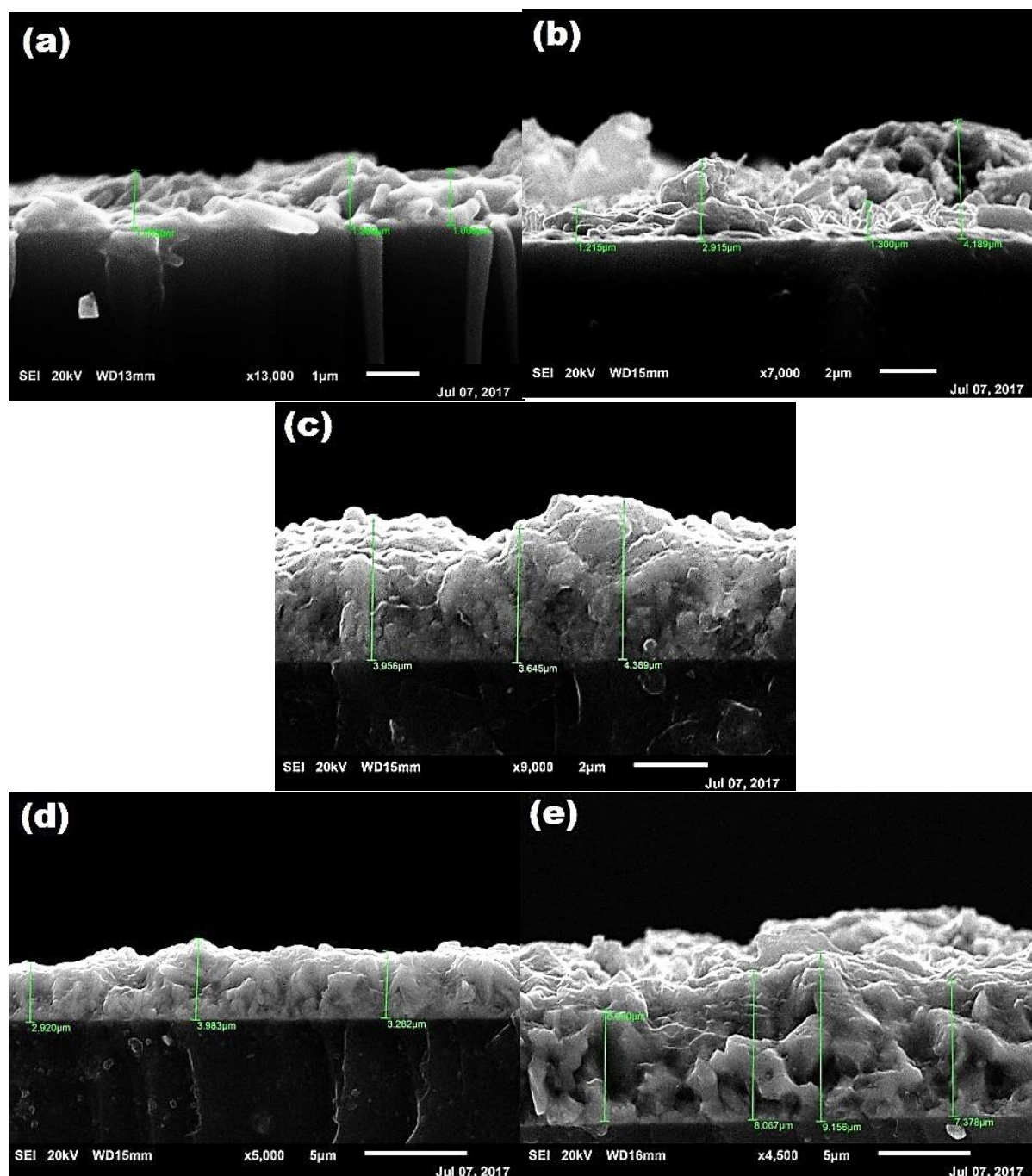


Figure 3. Cross-sectional SEM micrographs of variation in precursor concentration ZnO thin films.

Optical transmittance spectra recorded in the wave length range 200–1200 nm. For all thin films prepared at various precursor concentrations. Transmission spectra of all the ZnO thin films are shown in figure 4. The optical transmission spectrum shows that transmission decreases with increase in the concentration and the maximum transmission in visible region is about 54% for ZnO films prepared with 0.3 M and minimum transmission is about 33% with 0.5 M.

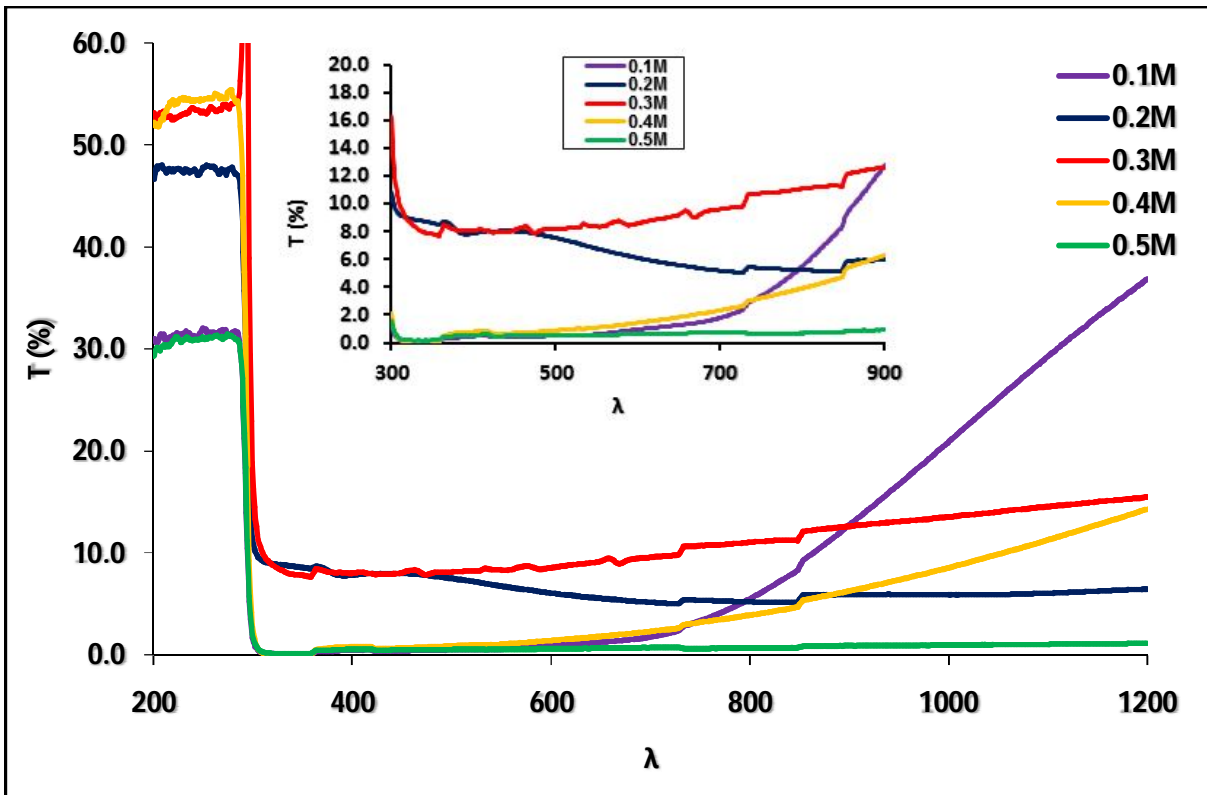


Figure 4. Transmittance spectra of variation in precursor concentration ZnO thin films.

Table 1 Structural, morphological and optical parameters for the multilayer ZnO thinfilms.

Variation in concentration	Crystallite size D (nm)	Average value of E	Thickness of film (μm)	Band gap Eg (ev)	Refractive indices at 550 nm	Extinction coefficients at 550 nm	Average of δ value (lines/m <sup>2</sup> )
0.1M	233	5.00X10 <sup>-3</sup>	1.14	3.37	1.04	1.12 X 10 <sup>-4</sup>	18.42
0.2M	238	4.43X10 <sup>-3</sup>	1.81	3.46	1.03	5.90 X 10 <sup>-3</sup>	17.65
0.3M	228	5.17X10 <sup>-3</sup>	3.99	3.47	1.03	5.44 X 10 <sup>-3</sup>	19.23
0.4M	218	5.40X10 <sup>-3</sup>	4.67	3.43	1.04	9.88 X 10 <sup>-3</sup>	21.04
0.5M	184	6.02X10 <sup>-3</sup>	10.2	3.36	1.04	11.3 X 10 <sup>-4</sup>	29.53

Absorbance was calculated from the Pankove relationship <sup>[16]</sup> as below.

$$A = \log\left(\frac{1}{T}\right) \tag{5}$$

Figure 5 shows the absorption spectra of grown films.



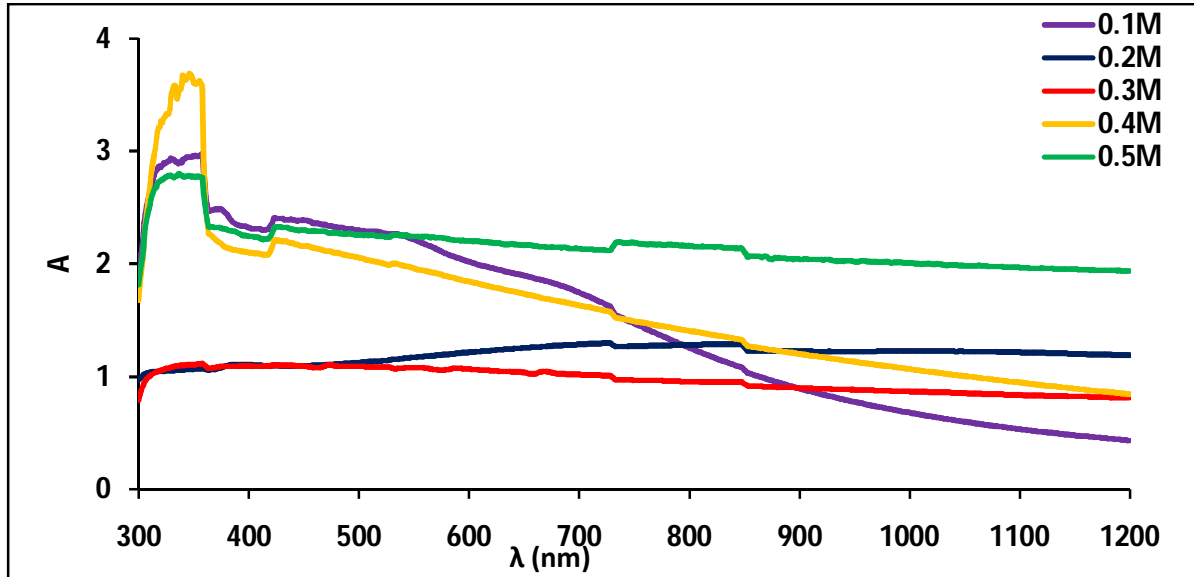


Figure 5. Absorbance spectra of variation in precursor concentration ZnO thin films.

The absorbance versus wavelength for ZnO thin films with different concentrations were shown in Fig. 5. The absorbance near 350 nm were sharp, the bend near the absorption edge confirms the polycrystalline structure of ZnO thin films. As we can see that the absorption in the visible and near IR remains almost constant. Absorbance of thin films are found to increase with increase concentration because of increase in thickness as well as increase in height of hexagonal pillars which forces incident radiation to suffer multiple reflections between their vertical surfaces. It is observed in figure 5 that the absorbance is very high up to ~350 nm and falls rapidly with increasing wavelength indicating the absorption edge in this region for all thin films. The absorption coefficient is obtained from the relation <sup>[16]</sup>;

$$\alpha = \frac{2.303A}{t} \quad (6)$$

Where *t* is the thickness of thin films obtained from cross-sectional SEM. Optical band gap of thin films were determined by plotting  $(\alpha h\nu)^2$  as a function of  $h\nu$ , and extrapolating the linear portion of the curve to  $(\alpha h\nu)^2=0$  as shown in fig. 7, using the formula <sup>[16]</sup>.

$$\alpha = \left(\frac{A}{h\nu}\right) (h\nu - E_g)^n \quad (7)$$

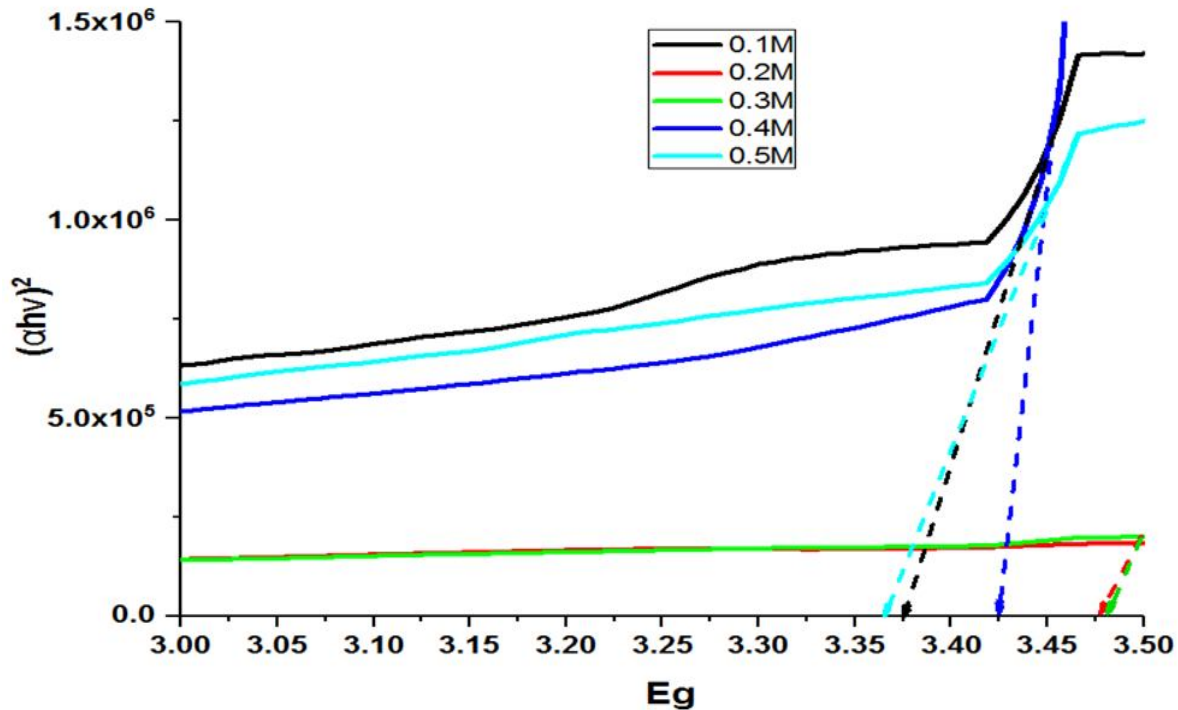


Figure 6. Plot of  $(\alpha hv)^2 \rightarrow hv$ , for ZnO multilayer thin films.

It is clear from figure 6 that the direct band gap values for all thin films are lying between 3.34-3.37 eV. Refractive indices of all thin films are calculated using the relation reported by Islam and podder [17].

$$n = \left( \frac{1+R}{1-R} \right) \quad (8)$$

Where  $n$  is the refractive index and  $R$  is the optical reflectance.

Values of direct band gap, refractive indices at 550 nm and extinction coefficients at 550 nm for all ZnO thin films are shown in Table 1.

## CONCLUSION

In summary, pure ZnO films have been successfully synthesized via chemical bath deposition method on glass substrates. ZnO nanostructure were successfully synthesized by a low cost not require high technology equipment's simple one step and without catalyst or buffer layer on substrate before the reaction chemical method, with high quality product. Structural, optical and morphological studies were carriedout. XRD data confirmed that the ZnO thin films were highly oriented along the (100), (002), (101), (102), (110), (103) and (200) plane. The sharp peaks show good crystallinity, resulting in high quality films. ZnO nanoparticles with average crystallite size of 184-233 nm were successfully synthesized via aqueous chemical route. As the concentration of the precursor increases, thickness of the film is increases and lattice strain is also increases gradually.

Transmittance spectra showed that transparency of the films ranged from 33 to 54%. The band gap energies from  $E_g = 3.36$  eV to 3.47 eV with intensive ultraviolet (UV) emission was concluded with increasing concentration from 0.1M to 0.5M. The crystallite size and band gap energy were found to depend on the concentration. The band gap increased as the crystallite size increased. The bath temperature was found to influence the growth of ZnO crystallites: at temperatures above 70 °C, good crystalline film was produced. The pH 9.6 was found to be the most suitable for CBD growth of ZnO.

## REFERENCES

- [1] Wei A, Pan L, Huang W, "Recent progress in the ZnO nanostructure-based sensors", *Materials Science and Engineering B*.2011; 176(18): 1409-1421.
- [2] Özgür U, Alivov Ya I, Liu C, et al, "A comprehensive review of ZnO materials and devices", *Journal of Applied Physics*.2005; 89(4): 041301.
- [3] Yevtushenko A I, Lashkaryov G V, Lazorenko V I, Karpina V A, Khranovskiy V D, "ZnO - UV detectors", *Physics and Chemistry of Solids*.2008; 9: 869-882.
- [4] Scheer R, Werner Schock H, *Chalcogenide Photovoltaics. Physics, Technologies, and Thin Film Devices*, Wiley-VCH, Weinheim. 2011; 175-192.
- [5] Rogozin I V, "Preparation of ZnO:N films by radical-beam gettering epitaxy method", *Semiconductor Physics and Technology*.2007; 41(8): 904-908.
- [6] Tuomisto F, Saarinen K, Grasza K, Mycielski A, "Observation of Zn vacancies in ZnO grown by chemical vapor transport", *Phys. stat. sol.*2006(4); 243: 794-798.
- [7] Chitanu E, Ionita Gh, "Obtaining thin layers of ZnO with magnetron sputtering method", *International Journal of Computers*.2010; 4(4): 243-250.
- [8] Bougrine A, Hichou A E, Addou M, Ebothé J, Kachouane A, Troyon M, "Structural, optical and cathodoluminescence characteristics of undoped and tin-doped ZnO thin films prepared by spray pyrolysis", *Materials Chemistry and Physics*.2003; 80(2): 438-445.
- [9] Kumari V, Malik B P, Mohan D, Mehra R M, "Laser Induced Nonlinear Optical Properties of Zinc Oxide Thin Film Prepared By Sol-Gel Method", *J. Nano- Electron. Phys.*2011; 3(1): 601-609.
- [10] Wang H, Xie C, "Controlled fabrication of nanostructured ZnO particles and porous thin films via a modified chemical bath deposition method", *Journal of Crystal Growth*.2006; 291(1):187-195.
- [11] Sankarpal B R, Sartale S D, Lokhande C D, and Ennoui A, Chemical synthesis of Cd-free wide band gap materials for solar cells, *Sol. Energy Mater. Solar Cells*.2004; 83(4):.447
- [12] Kathirvel P, Manoharan D, Mohan S M, and Kumar S, Spectral Investigations of Chemical Bath Deposited Zinc Oxide Thin Films–Ammonia Gas Sensor, *J. Optoelectronic and Biomedical Materials*.2009; 1: 25.

- [13] Kalita P K, Sarma B K and Das H L, Photoresponse characteristics of vacuum evaporated ZnTe thin films, Indian J. Pure & Appl. Phys. 1999;37(12): 885.
- [14] Shikzlgar A G, and Pawar S H, Photoconducting properties of cadmium sulphide-lithium thin films formed by the chemical bath deposition method, Thin Solid Films.1979; 61(3):313-320.
- [15] Forouhi A R, Bloomer I. "Optical Dispersion Relations for Amorphous Semiconductors and Amorphous Dielectrics". Physical Review B.1986; 34 (10): 7018–7026.
- [16] Pankove J I, Optical Processes in Semiconductors.1971; 3:1338.
- [17] Bao D, Gu H, Kuang A, Thin Solid Films.1988; 312(1-2): 37-39.
-